Program Digest, 2019 IEEE International Ultrasonics Symposium (IUS)
Glasgow, Scotland, October 6-9, 2019

Force-Map Normalization for ARFI Imaging

Peter Hollender
Biomedical Engineering
Duke University
Durham, NC USA
peter.hollender@duke.edu

Souhaila Noor
Biomedical Engineering
Duke University
Durham, NC USA
souhaila.noor@duke.edu

David Bradway
Biomedical Engineering
Duke University
Durham, NC USA
david.bradway@duke.edu

Gregg Trahey
Biomedical Engineering
Duke University
Durham, NC USA
gregg.trahey@duke.edu

***Abstract*—Acoustic Radiation Force Impulse (ARFI) images are used to visualize spatial variations in soft tissue elasticity by showing the displacement of each pixel in response to an applied radiation force. However, accommodations for spatial variations in the applied radiation force itself have been limited. When imaging a phantom, reference lines that contain no targets can be used to calibrate the depth-dependence of the applied force, but this is not feasible in vivo. We present here a method of estimating the spatially-varying applied force map via automatic segmentation of the matched B-Mode image, and use these maps to normalize ARFI image to have decreased spatial variability.**

Keywords—Acoustic Radiation Force, Elastography, Intracardiac Echocardiography

I. INTRODUCTION

Acoustic Radiation Force Impulse (ARFI) imaging[1] has shown promise for visualizing radiofrequency ablation (RFA) lesions in the left atrium using an intracardiac echocardiography (ICE) catheter-tip array[2]–[4]. While the small size of the steerable array affords direct views of the myocardium from within the atrium, it also leads to significant spatial gradients in the generated ARFI displacement images, owing to the nonuniform distribution of acoustic radiation force (ARF). In most organs, overlying tissue adds reverberation, clutter and attenuation of an unknown magnitude. For ICE ARFI, the acoustic path to any pixel is greatly simplified to be partially hypoechoic and low-attenuating blood, and the rest echogenic and attenuating myocardium, with the contrast between the two visible on B-Mode. We demonstrate here that for known, two-phase acoustic paths, the relative ARF field can be estimated and used to suppress the image-specific gradients created by these two effects. The experiment presented here in uniform phantoms lays the initial groundwork for application to heterogenous targets and *in vivo* images in future work.

II. METHODS

A. Experimental Setup

ARFI images were collected on a Siemens SC2000 ultrasound scanner using an AcuNav 8F ICE array. Five CIRS Zerdine phantoms of different elasticities were imaged, using clinical imaging sequences used for previously published intracardiac ARFI studies. The sequences used 30 pushes varying between -22.5 and 22.5 degrees, with a focal depth of 15 mm and a maximum imaging depth of 20mm. The array was secured to a metal fixture attached to a 4-axis translation stage (xyz + rotation about the y-axis). The stage was used to vary the distance between the transducer tip and the phantom between 5 and 11 mm in 1 mm increments, the angle of the phantom surface in the imaging plane between 0 and 10 mm in 1 mm increments, and the elevational position in 5, 1.5 mm increments to obtain independent speckle realizations.

B. Approximation of Geometry

From each acquired B-Mode, the image was segmented into water and phantom regions. To do so, the dynamic range of the B-Mode was reduced, then each B-Mode image (195 pixels in depth, 30 in angle) was filtered with a 5x5 median filter. After pre-processing, a 1-D (-1,1) step function kernel of 5 mm in length was convolved with each column to detect the transition between the water (dark) and the phantom (bright). The boundary location was identified on each column of the B-Mode image independently

C. Displacement Estimation

Displacement estimation was performed with Loupas' algorithm[5] and a 5-lambda kernel. An extrapolation linear motion filter was applied to each displacement trace using the 1 ms (8 samples) of reference lines to remove background motion. The ARFI displacement was then taken as the displacement 1 ms following the ARFI excitation.

D. Building the Force Library

The magnitude of acoustic radiation force is well known as

$$F = 2\alpha I/c$$

Where F is the force, α is the attenuation coefficient, I is the time-integrated intensity of the applied pulse, and c is the speed of sound. We will assume for the water-phantom experiments that alpha is 0.5 db/cm/MHz in the phantom and 0dB in water (in blood, it would be 0.15 dB/cm/MHz). The speed of sound is assumed to be constant at 1540 m/s in the phantom. With such assumptions, radiation force is applied to the phantom in a spatial distribution consistent with the intensity field, and scaled in a binary manner by whether each pixel is water or phantom. Thus, we make the assumption that by measuring the displacements in uniform

Identify applicable funding agency here. If none, delete this text box.

phantoms of elasticities, the displacements will be inversely proportional to elasticity, and will show an elasticity-independent spatial pattern reflecting the relative applied intensity.

To create lookup tables, the median displacement in each non-rotated image over of the 5 speckle realizations was taken. Then, each image was normalized by the maximum displacement along the center steering angle. Finally, the normalized images were averaged across all 5 elasticities to provide the consensus shape of the "force" map at each boundary depth, assuming that any spatial variation in displacement can be attributed to variations in the spatial force applied, as the phantoms are nominally uniform.

E. Estimating relative Applied Force and applying Normalization

Using each B-Mode image, the geometry approximation was used to find the distance to the phantom surface at each angle. This distance was used to select from the lookup maps which boundary depth to use, and the relative force amplitude for the corresponding ARFI beam angle was extracted. The process is repeated for each steering angle until the entire image is built. To apply the normalization, the ratio of the estimated force to the displacement (an estimate of elasticity), or its reciprocal (an estimate of compliance) are alternately used to create the final maps. Furthermore, no displacements are shown above the detected boundary, or in distal hypoechogenic regions, where the attenuation of the ultrasound signal has been so great that no signal to noise ratio remains on the displacements.

III. RESULTS

Figure 1 shows an example of the process of displacement normalization. The displacement/force maps are more uniform in appearance than the raw displacement maps, and maintain the same contrast between elasticities.

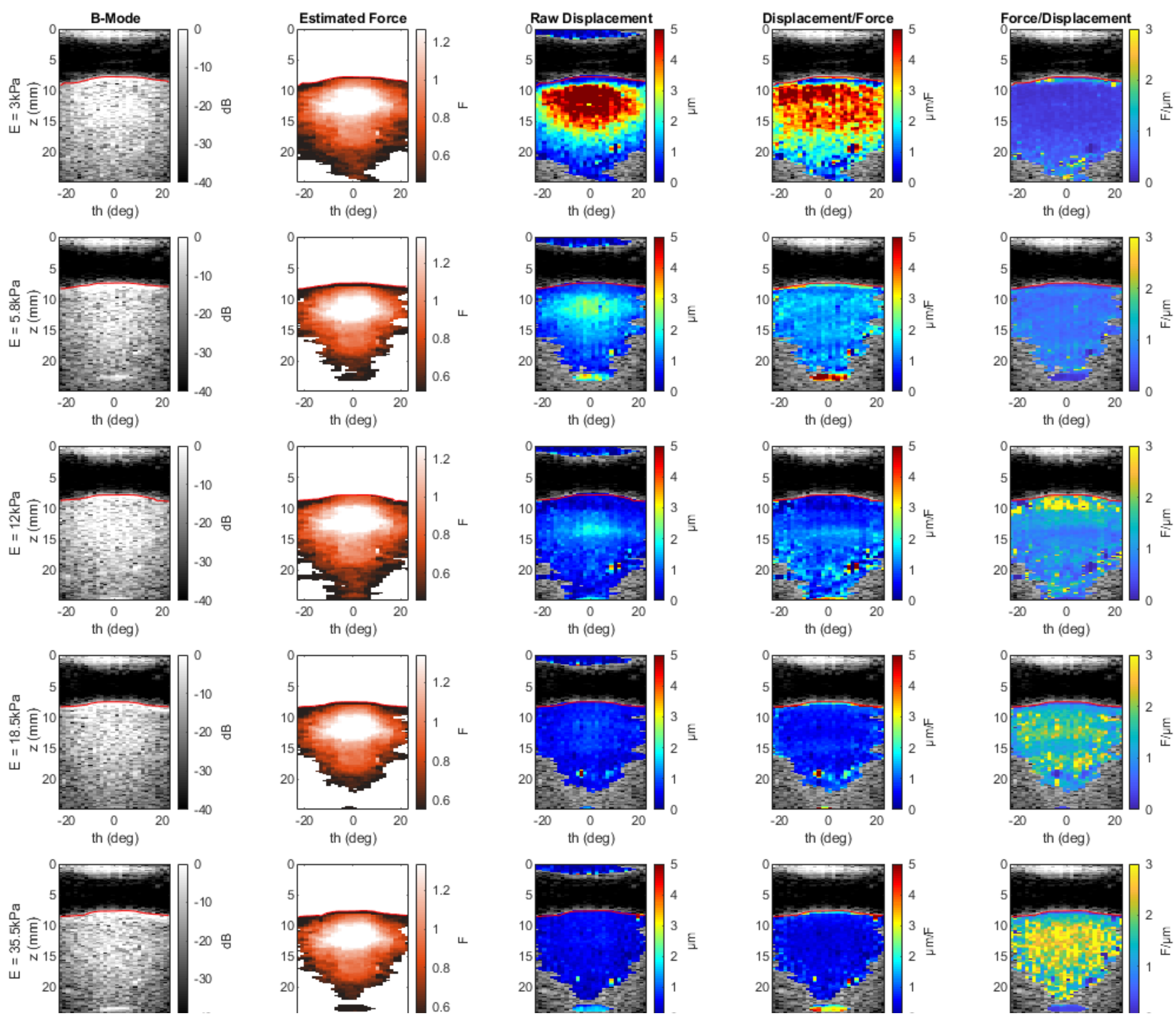

Figure 1: Example of the normalization Process. The B-Mode image is used to construct an estimated force map from the library, which is used to normalize the spatial distribution of the gradients.

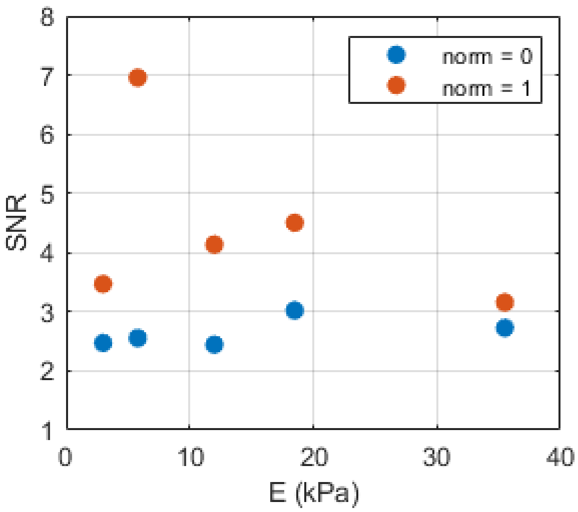

Figure 2: Signal to noise ratio (SNR) of displacement images with and without normalization. Normalization results in a 15% - 170% increase in SNR.

Figure 2 shows the signal-to-noise ratio (SNR) increase across all elasticities. SNR is the ratio of the mean to the standard deviation. In all cases, the SNR is improved with force map normalization.

Figure 3 shows the performance of the algorithm at correcting for imaging steering angles. The boundary detection continues to detect the angled top surface of the phantom correctly, and the normalized displacement maps have a uniform spatial appearance.

IV. Discussion

A. Utility

The primary envisioned use of this technique is for intracardiac imaging. Unlike abdominal imaging, where the specific acoustic attenuation of each layer is unknown, in intracardiac echocardiography, we can reasonably assume that the path along which any radiation force beam travels is comprised of either blood or heart tissue. In this way, the echogenicity of the B-Mode image can be used to create an image-specific normalization map for the ARFI displacements. Such normalization may improve the visual conspicuity of spatial targets, as the endogenous contrast owing to variably-applied force will be removed.

B. Next Steps

The algorithm needs to be tested on phantoms with elasticity contrast targets, phantoms with more complex geometry, and finally *in vivo* images of cardiac tissue. Furthermore, the algorithm could be refined and improved with a pixel-based approach to force estimation as opposed to the beam-based approach employed here. By comparing the section of the B-mode encompassed by a triangle formed by the two edges of the aperture and the focal point to similar triangles in the lookup table for the same focal configuration, a per-pixel estimate of intensity can be estimated that varies with more complex geometry than the simple boundary used here.

C. Limitations

Our originally-conceived approach was to use FullWave[6] to simulate the propagation of the acoustic waves into a two phase simulated medium to obtain a large library of *in silica* intensity fields. However, the complex shear propagation after induced displacement created spatial differences between simulated intensity fields and measured ARFI displacements in uniform media. A modification to the method of forming ARFI images or to the method of simulation to match the experimental observations may enable such a process in the future. Furthermore, while the dataset collected here was fairly large (25 GB), the distances and angles are hardly comprehensive to be able to stitch together the complex geometries present in the heart, and were all performed for a single focal configuration. A new

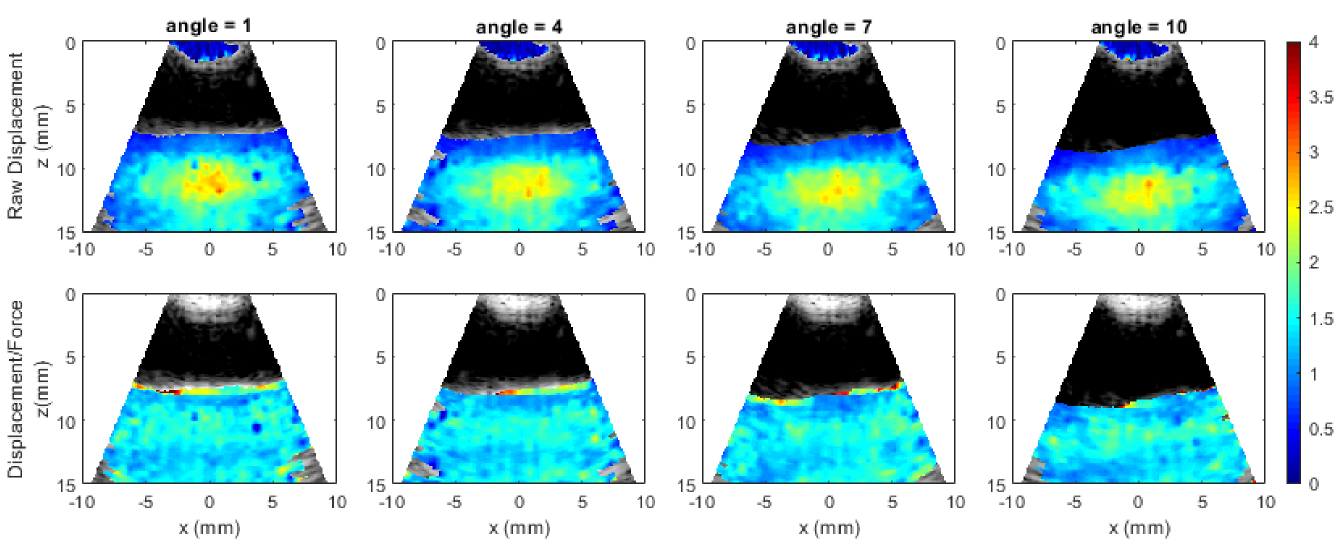

Figure 3: Force map normalization for different steering angles. The phantom appears uniform at different imaging angles, even though the lookup table only used the flat boundaries.

look-up table would be required for each unique set of acquisition parameters.

V. Conclusion

In this work, we demonstrated a concept for estimating the relative force applied to different locations in an ARFI image, and using it to normalize ARFI maps. This method reduces the spatial variation within the maps, and in future work may enable improved visualization of contrast targets.

VI. References

[1] M. L. Palmeri, S. A. McAleavey, K. L. Fong, G. E. Trahey, K. R. Nightingale, and S. Member, "Dynamic mechanical response of elastic spherical inclusions to impulsive acoustic radiation force excitation.," IEEE Trans Ultrason Ferroelectr Freq Control, vol. 53, no. 11, pp. 2065–2079, Nov. 2006.

[2] P. J. Hollender, P. D. Wolf, R. Goswami, and G. E. Trahey, "Intracardiac Echocardiography Measurement of Dynamic Myocardial Stiffness with Shear Wave Velocimetry," Ultrasound Med. Biol., vol. 38, no. 7, pp. 1271–1283, 2012.

[3] P. D. Wolf et al., "Near Real Time Evaluation of Cardiac Radiofrequency Ablation Lesions with Intracardiac Echocardiography Based Acoustic Radiation Force Impulse Imaging," Present. 161st Meet. Acoust. Soc. Amer., J. Acoust. Soc. Amer., vol. 129, no. 4, p. 2438, 2011.

[4] S. J. Hsu, B. J. Fahey, D. M. Dumont, P. D. Wolf, and G. E. Trahey, "Challenges and implementation of radiation-force imaging with an intracardiac ultrasound transducer.," IEEE Trans Ultrason Ferroelectr Freq Control, vol. 54, no. 5, pp. 996–1009, May 2007.

[5] T. Loupas, R. Peterson, and R. Gill, "Experimental Evaluation of Velocity and Power Estimation for Ultrasound Blood Flow Imaging, by Means of a Two-Dimensional Autocorrelation Approach," IEEE Trans. Ultrason. Contr., vol. 42, no. 4, pp. 689–699, 1995.

[6] G. Pinton, "Three dimensional full-wave nonlinear acoustic simulations of ultrasound imaging and therapy in the entire human body."